

Direct High-Power Laser Acceleration of Ions for Medical Applications

Yousef I. Salamin,^{1,2,*} Zoltán Harman,^{1,†} and Christoph H. Keitel^{1,‡}

¹*Max-Planck-Institut für Kernphysik, Saupfercheckweg 1, 69117 Heidelberg, Germany*

²*Physics Department, American University of Sharjah, POB 26666, Sharjah, United Arab Emirates*

Theoretical investigations show that linearly and radially polarized multiterawatt and petawatt laser beams, focused to subwavelength waist radii, can directly accelerate protons and carbon nuclei, over micron-size distances, to the energies required for hadron cancer therapy. Ions accelerated by radially polarized lasers have generally a more favorable energy spread than those accelerated by linearly polarized lasers of the same intensity.

PACS numbers: 52.28.Kd, 37.10.Vz, 42.65.-k, 52.75.Di

Protons and heavier ions are now being used to treat cancer at a number of places around the world [1]. Ion lithography schemes seem to be heading for practical application [2] and fusion research continues to attract considerable attention and to gain in importance [3]. In addition, considerable effort is being devoted to research into the fundamental forces of nature, the initiation of nuclear reactions and into schemes to treat radioactive waste [4]. In these applications, conventional accelerators (synchrotrons, cyclotrons and linacs) are employed which are large and expensive to build and operate.

To produce and accelerate ions, current plasma-based research focuses on the use of thin foils irradiated by femtosecond laser pulses of intensity $> 10^{18}$ W/cm² [5]. Typically a laser pulse is incident on the thin foil giving rise to an overdense plasma from which the electrons get accelerated, form a dense sheath on the opposite side and generate a quasistatic electric field of strength in excess of 10^{12} V/m. This superstrong field accelerates the ions to tens of MeV over a distance in the μm range [6]. Recent work [7] has shown that proton beams produced by this method of target normal sheath acceleration (TNSA) may be improved in energy and beam quality by the use of foils less than $1 \mu\text{m}$ in thickness [8]. In earlier experiments, employing thicker foils, a small fraction of the energy got converted to proton energy. Furthermore, the protons had energy spreads reaching 100%.

In hadron therapy [9, 10, 11], for example, the ions are required to have kinetic energies $K = 20 - 250$ MeV/nucleon (H^+ and He^{2+}) and $K = 85 - 430$ MeV/nucleon (C^{6+} and O^{8+}). The ions also ought to have an energy spread $\Delta K_f / \bar{K}_f < 1\%$ so that they may be focused on the tumor while sparing the neighboring healthy tissue. A beam of rectangular cross section is also desirable [11].

In this Letter we study direct laser acceleration configurations of protons and bare carbon nuclei. The aim is to make predictions regarding the optimum conditions that would lead to the ion energies of interest to hadron therapy. A source for the ions may be a dedicated electron beam ion trap/source (EBIT/EBIS) [12] from which they can be extracted in a well-defined fully ionized charge

state or an ensemble of fully stripped ions produced by laser-solid interaction. We consider a situation in which the source has been tailored on a nanoscale [9, 13]. We study the dynamics of an ensemble of N particles having normally distributed kinetic energies, using the single-particle relativistic Lorentz-Newton equations. Our calculations show that laser pulses generated by 0.1–10 PW laser systems accelerate ions directly to energies in the ranges required for hadron therapy, provided the laser beams are focused to subwavelength waist radii. The accelerated ions turn out to have high beam quality and rectangular and circular cross sections reflecting symmetry of the field and shape of the initial ionic distribution.

Key to generating the ultrastrong accelerating fields is focusing the laser beam to a subwavelength waist radius. According to recent experiments, a linearly polarized beam of wavelength λ may be focused to a spot of size $(0.26\lambda)^2$, where the spot size is the area enclosed by a contour at which the beam intensity falls to one half its peak value. A radially polarized beam may be focused to the substantially smaller spot size of $(0.16\lambda)^2$ [14].

Upon tight focusing, a linearly polarized laser beam develops five field components. The nonvanishing field components of a beam polarized along the x axis, propagating along the z axis, of wavelength λ and frequency ω , are given in [15], using the familiar Gaussian-beam parameters (waist radius w_0 , Rayleigh length $z_r = \pi w_0^2 / \lambda$ and diffraction angle $\varepsilon = w_0 / z_r$). The laser power expression may be given, to order ε^{10} , by

$$P_l = \frac{\pi w_0^2 E_{0l}^2}{4 c \mu_0} \left[1 + \left(\frac{\varepsilon}{2}\right)^2 + 2 \left(\frac{\varepsilon}{2}\right)^4 + 6 \left(\frac{\varepsilon}{2}\right)^6 + \frac{45}{2} \left(\frac{\varepsilon}{2}\right)^8 + \frac{195}{2} \left(\frac{\varepsilon}{2}\right)^{10} \right], \quad (1)$$

where μ_0 is the permeability of free space, E_{0l} is the electric field amplitude, c is the speed of light in vacuum and the subscript l stands for linearly polarized. Note that $E_{0l} \propto \sqrt{P_l}$ and that the leading term in E_{0l} is inversely proportional to w_0 .

Dynamics of a particle of mass M and charge Q in electric and magnetic fields is governed by the equations

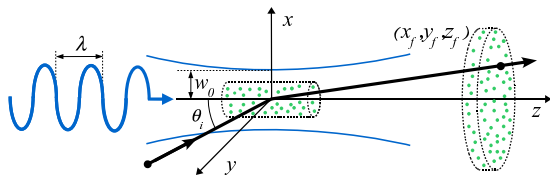


FIG. 1: (Color online) Schematic geometry of the acceleration scenario. The initial coordinates of the ions are randomly distributed in a cylinder which models the interaction regime of the ion beam and the laser field. The ejected ions then form a beam of circular cross section when the ions are accelerated

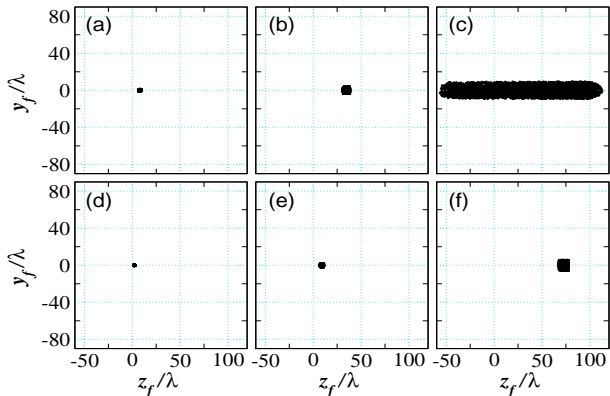


FIG. 2: (Color online) Coordinates (z_f, y_f) of 5000 particles at the end of their trajectories after interaction with linearly polarized light. (a)-(c) are for protons ${}^1\text{H}^+$ and (d)-(f) are for carbon nuclei ${}^{12}\text{C}^{6+}$. The parameters are: $\lambda = 1054$ nm, $w_0 = 0.5\lambda$. The equations have been integrated over a time interval equivalent to 1000 laser field cycles, approximately amounting to 3.516 ps. For further data see Table I.

of motion

$$\frac{d\mathbf{p}}{dt} = Q[\mathbf{E} + c\boldsymbol{\beta} \times \mathbf{B}]; \quad \frac{d\mathcal{E}}{dt} = Qc\boldsymbol{\beta} \cdot \mathbf{E}, \quad (2)$$

in which the energy and momentum of the particle are given by $\mathcal{E} = \gamma Mc^2$ and $\mathbf{p} = \gamma Mc\boldsymbol{\beta}$, respectively, with $\boldsymbol{\beta}$ its velocity scaled by c , and $\gamma = (1 - \beta^2)^{-1/2}$ its Lorentz factor. Integrating Eqs. (2) numerically one obtains $\boldsymbol{\beta}$ and, hence, γ_f at a later time t_f taken equal to many laser field cycles. The final kinetic energy is $K_f = (\gamma_f - 1)Mc^2$.

To model the interaction region of the ion beam and the laser we consider an ensemble of $N = 5000$ particles initially randomly distributed in a cylinder of radius $R_c = 10$ nm and length $L_c = 100$ nm oriented along the z axis and centered on the origin (see Fig. 1). In order to simulate a realistic ion beam extracted from some ion source, the particles will be assumed to possess Gaussian distributed random initial kinetic energies with a mean value $\bar{K} = 10$ keV and a spread $\Delta K = 10$ eV. Initial direction of motion of all particles will be in the xz plane and at $\theta_i = 10^\circ$ relative to the pulse propagation direction.

All \mathbf{E} components, together with the $\mathbf{v} \times \mathbf{B}$ force, work to accelerate a particle and deflect it to varying degrees from its initial direction of motion [15]. A particle makes the longest excursion along the x axis due to E_x being the strongest accelerating component, smaller excursions occur due to E_y and E_z . An ensemble of such particles forms a beam of rectangular cross section in the yz plane, reflecting symmetry of the laser field. This is demonstrated in Fig. 2 for interaction with 0.1, 1 and 10 PW laser beams. The ion beam cross section increases with increasing laser power ($E_{0l} \propto \sqrt{P_l}$). The transverse proton beam divergence is larger than for carbon. Energy gain by protons is also greater than the gain per nucleon of carbon, due to the proton's larger charge to mass ratio. Further data not estimable from Fig. 2 are collected in Table I. Note that the energies fall within the domain required for hadron therapy and their spread is close to what would be suitable for such a purpose. Our calculations also show that the relative energy spread tends to increase approximately linearly with the volume of the initial ionic distribution. However, the input (and output) particle beam may be collimated using externally applied electromagnetic fields (see, e.g. Ref. [16]).

For realization, a short pulse consisting of only a small number of field cycles would be needed. This conclusion is elucidated by showing, in Fig. 3 for a typical member of the ensemble, the particle kinetic energy as a function of the number of interaction cycles. The number of actual interaction field cycles is small and decreases with increasing power, since ions accelerated to higher velocities leave the focal region faster. Laser-to-particle energy conversion occurs in the form of a few violent impulses. Note also that, due to its lower velocity, a carbon ion interacts with more field cycles than a proton.

Estimates may be obtained for the transverse and longitudinal emittances ϵ_T and ϵ_L , respectively, of the particle beam. Using ensemble averages of the exit particle coordinates and kinetic energies, one calculates $\epsilon_T < 10\pi$ mm mrad and $\epsilon_L < 4 \times 10^{-5}$ eV s for protons (case of Fig.

TABLE I: Data related to Fig. 2. Laser power, average particle final x coordinate \bar{x}_f , average final kinetic energy \bar{K}_l and relative kinetic energy spread $\Delta K_l/\bar{K}_l$ at the end of the trajectories of protons, (a)-(c), and carbon nuclei, (d)-(f). The ions are interacting with linearly (l) polarized light.

	Power [PW]	\bar{x}_f [λ]	\bar{K}_l [MeV/nucleon]	$\Delta K_l/\bar{K}_l$ [%]
(a)	0.1	89.6 ± 0.6	3.77 ± 0.05	1.3
(b)	1	283.0 ± 1.7	37.39 ± 0.45	1.2
(c)	10	750.6 ± 41.1	416.5 ± 24.7	5.9
(d)	0.1	44.9 ± 0.3	0.94 ± 0.01	1.2
(e)	1	141.3 ± 0.9	9.32 ± 0.11	1.2
(f)	10	434.3 ± 2.5	89.9 ± 0.9	1.0

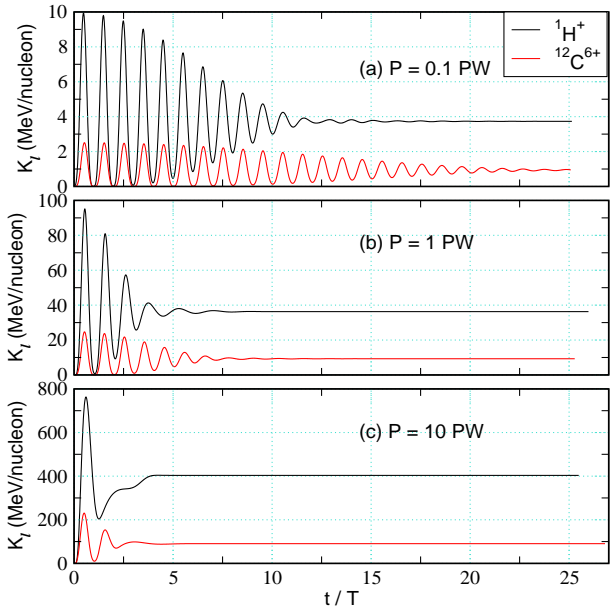


FIG. 3: (Color online) Kinetic energy of a typical particle (out of the ensembles of Fig. 2) during interaction with linearly polarized light. In the figure, T is one laser field period.

2(c)). A comparison of these figures with results recently reported for ion beams produced from ultrathin solid foils irradiated by multiterawatt and petawatt linearly polarized laser beams [13, 17] reveals that a good quality proton beam may be obtained by direct laser acceleration. Estimates for carbon yield $\epsilon_T < 0.3\pi$ mm mrad and $\epsilon_L < 9 \times 10^{-6}$ eV s (case of Fig. 2(f)). The remaining cases in Fig. 2 have better emittances.

A Gaussian beam of linear polarization is relatively easy to generate in the laboratory, while the same thing may not be said about a beam of the radially polarized variety. The electric field of a radially polarized focused (axicon) laser beam has two components, radial E_r and axial E_z , with propagation along the z axis. However, only one azimuthally polarized magnetic field component, B_θ , exists. E_z works efficiently to accelerate the particles, while E_r and B_θ help to limit their diffraction [18, 19]. Full expressions for the axicon field components are given in [20]. The power of the axicon beam, to order ϵ^{10} , reads

$$P_r = \frac{\pi w_0^2 E_{0r}^2}{2 c \mu_0} \left(\frac{\epsilon}{2}\right)^2 \left[1 + 3 \left(\frac{\epsilon}{2}\right)^2 + 9 \left(\frac{\epsilon}{2}\right)^4 + 30 \left(\frac{\epsilon}{2}\right)^6 + \frac{225}{2} \left(\frac{\epsilon}{2}\right)^8 \right]. \quad (3)$$

Note that the amplitude $E_{0r} \propto \sqrt{P_r}$. On the other hand, when the definition of ϵ is used, one finds that the leading term in E_{0r} is independent of w_0 . While E_{0l} has a peak value beyond which it falls asymptotically to zero, with increasing w_0 , E_{0r} increases to an asymptotic value.

Figs. 4 and 5 are similar to Figs. 2 and 3, respectively, albeit for particle acceleration by radially polarized laser

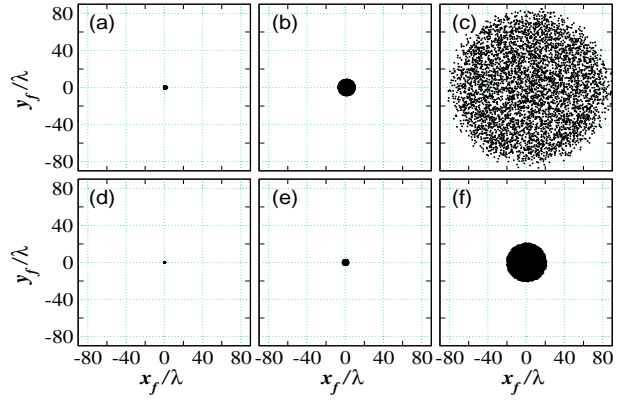


FIG. 4: (Color online) Same as in Fig. 2, for particles accelerated by radially polarized light. For further data see Table II.

fields. From Fig. 4 one sees that the particle beam cross section in the xy plane is almost circular, reflecting symmetry of the initial distribution. Recall that the radial electric field component E_r vanishes on the beam axis and its magnitude at a typical particle trajectory is smaller than the transverse field in the linearly polarized case. In addition, E_r plays a confining role during the half-cycle in which it is radially inward and tends to cause dispersion during the following half cycle. The fact that most of the beam power is concentrated in E_z , due to tight focusing, is also responsible for the extra energy gain from the radially polarized beam compared to that obtained from a linearly polarized one. Comparison of Figs. 5 and 3 also shows that a particle, since it is confined to dominantly axial motion, interacts with many more radially polarized cycles than it does with linearly polarized ones.

To assess the beam qualities, estimates show that, for protons, $\epsilon_T < 3\pi$ mm mrad and $\epsilon_L < 4 \times 10^{-5}$ eV s (case of Fig. 4(c)), while for carbon $\epsilon_T < \pi$ mm mrad and $\epsilon_L < 4 \times 10^{-6}$ eV s (case of Fig. 4(f)). The remaining cases in Fig. 4 have better emittances. These results are several orders of magnitude lower than their counterparts in conventional accelerators. They are also comparable to, and sometimes even better than, the corresponding figures for ion beams produced from ultrathin foils [13,

TABLE II: Data related to Fig. 4. Same as Table I, for ions interacting with radially (r) polarized light.

	Power [PW]	\bar{z}_f [λ]	\bar{K}_r [MeV/nucleon]	$\Delta K_r / \bar{K}_r$ [%]
(a)	0.1	104.7 ± 0.5	4.26 ± 0.03	0.7
(b)	1	430.8 ± 2.3	45.7 ± 0.4	0.8
(c)	10	3347.5 ± 89.6	532.8 ± 13.3	2.5
(d)	0.1	48.5 ± 0.2	1.00 ± 0.01	1
(e)	1	173.7 ± 0.8	10.4 ± 0.1	0.8
(f)	10	876.1 ± 5.3	122.0 ± 1.0	0.8

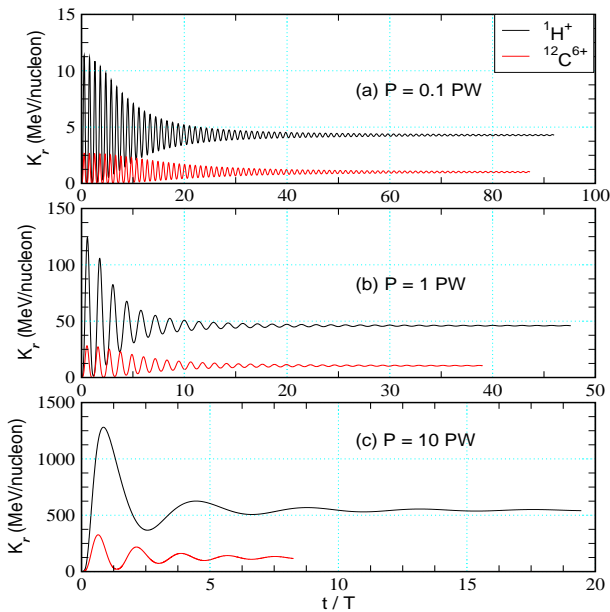


FIG. 5: (Color online) Kinetic energy of a typical particle (out of the ensembles of Fig. 4) during interaction with radially polarized light.

17].

The average kinetic energies gained from interaction with radially polarized laser beams are somewhat better than from interaction with the linearly polarized ones (compare Tables I and II). These energies, with their low spread, cover the domain of application in hadron therapy. Note that the initial ensemble volume corresponds to an ion density $n_i \sim 10^{20} \text{ cm}^{-3}$. Estimations of the energies transferred via space-charge effects suggest that those are negligible for the parameters applied. One could, in principle, start out with ensemble parameters that would lower this density down to $n_i \sim 10^{17} \text{ cm}^{-3}$ and still keep the accelerated beam quality within the limits of utility in ion therapy. Unfortunately, these densities are many orders of magnitude higher than what is available today from conventional ion sources. Further design improvements on such machines need to be made before they may be used as ion sources for direct acceleration. An alternative source could possibly be a solid target of micro- or nanoscale thickness, perhaps blown off by a laser pulse, as in the TNSA mechanism [7, 8] and the laser-piston regime [21], followed at the appropriate time delay by an accelerating pulse of the type discussed in this Letter.

In conclusion, direct laser acceleration of ions is put forward as an appealing alternative for utilization in cancer therapy. Radially polarized beams of the required power and intensity are not currently available. Employing an existing linearly polarized beam, on the other hand, may call for a focusing mechanism to bring the ion beam spreading down and render it useful in applications.

Z.H. acknowledges insightful conversations with José R. Crespo López-Urrutia.

* Electronic address: ysalamin@aus.edu

† Electronic address: harman@mpi-hd.mpg.de

‡ Electronic address: keitel@mpi-hd.mpg.de

- [1] S. Fritzier *et al.*, Appl. Phys. Lett. **83**, 3039 (2003); X. Peng *et al.*, Phys. Rev. E **74**, 036405 (2006); O. Jäkel *et al.*, Nucl. Instrum. Methods Phys. Res. B **241**, 717 (2005); <http://www.klinikum.uni-heidelberg.de/Heidelberger-Ionenstrahl>; http://www.gsi.de/portrait/beschleunigeranlage_e.html; <http://www.wanjiehospital.com/proton/program.htm>.
- [2] A. Alves *et al.*, Nucl. Instrum. Methods Phys. Res. B **249**, 730 (2006).
- [3] M. Roth *et al.*, Plasma Phys. Control. Fusion **47**, B841 (2005).
- [4] P. McKenna *et al.*, Phys. Rev. Lett. **91**, 075006 (2003); K. W. D. Ledingham, P. McKenna, and R. P. Singhal, Science **300**, 1107 (2003).
- [5] J. Badziak, Opto-electr. Rev. **15**, 1 (2007) and references therein; M. Hegelich *et al.*, Phys. Rev. Lett. **89**, 085002 (2002).
- [6] A. J. Mackinnon *et al.*, Phys. Rev. Lett. **86**, 1769 (2001); J. Fuchs *et al.*, Phys. Rev. Lett. **99**, 015002 (2007).
- [7] A. Maksimchuk *et al.*, Phys. Rev. Lett. **84**, 4108 (2000); S. Karsch *et al.*, Phys. Rev. Lett. **91**, 015001 (2003); L. Romagnani *et al.*, Phys. Rev. Lett. **95**, 195001 (2005); B. M. Hegelich *et al.*, Nature **439**, 441 (2006); H. Schwöerer *et al.*, Nature **439**, 445 (2006); R. A. Snavely *et al.*, Phys. Rev. Lett. **85**, 2945 (2000); T. E. Cowan *et al.*, Nucl. Instr. Meth. Phys. Res. **544**, 277 (2005); B. J. Albright *et al.*, Phys. Rev. Lett. **97**, 115002 (2006).
- [8] D. Neely *et al.*, Appl. Phys. Lett. **89**, 021502 (2006); P. Antici *et al.*, Phys. Plasmas **14**, 030701 (2007); A. P. L. Robinson and P. Gibbon, Phys. Rev. E **75**, 015401(R) (2007).
- [9] S. V. Bulanov *et al.*, Phys. Lett. A **299**, 240 (2002).
- [10] <http://www-aix.gsi.de/~spiller/therapie.html>.
- [11] H. Svensson and T. R. Möller, Acta Oncologica **42**, 430 (2003).
- [12] J. R. Crespo López-Urrutia *et al.*, J. Phys.: Conf. Ser. **2**, 42 (2004); T. Beier *et al.*, Nucl. Instr. Meth. Phys. Res. B **235**, 473 (2005).
- [13] M. Roth *et al.*, Opt. Commun. **264**, 519 (2006).
- [14] S. Quabis *et al.*, Appl. Phys. B **72**, 109 (2001); S. Quabis, R. Dorn, and G. Leuchs, Appl. Phys. B **81**, 597 (2005).
- [15] Y. I. Salamin, Appl. Phys. B **86**, 319 (2007); Y. I. Salamin and C. H. Keitel, Phys. Rev. Lett. **88**, 095005 (2002).
- [16] M. Verschl and C. H. Keitel, Europhys. Lett. **77**, 64004 (2007).
- [17] M. Roth *et al.*, Hyperfine Interactions **162**, 45 (2006).
- [18] M. O. Scully and M. S. Zubairy, Phys. Rev. A **44**, 2656 (1991).
- [19] I. Bialynicki-Birula, Phys. Rev. Lett. **93**, 020402 (2004).
- [20] Y. I. Salamin, New J. Phys. **8**, 133 (2006); Opt. Lett. **31**, 2619 (2006).
- [21] T. Esirkepov *et al.*, Phys. Rev. Lett. **92**, 175003 (2004).